

Supplementary figure legends

Figure S1. Characterization of Golgi de novo biogenesis after laser nanosurgery

A) Additional examples of analyses of the time-lapse imaging of Golgi de novo biogenesis. Karyoplasts were generated by laser nanosurgery and time-lapse imaging was performed and analyzed as in 2A with different time resolution (2-5-60minutes). The plots monitor the changes of the total cellular fluorescence intensity (F.I.) of the Golgi marker YT2 (black line) and the F.I. in segmented structures (red line) over time and show the bimodal kinetics of Golgi de novo biogenesis.

B) ER export inhibition during phase 1 is not specific for YT2. YT2 cells growing on patterned coverslips for 48h were infected with an adenoviral vector for the expression of GPI-CFP. After 1h incubation, cells were washed and left for 3h before nanosurgery. The karyoplast (asterisk) was then followed by 2 color time lapse imaging to monitor the behavior of the Golgi marker YT2 and of the other cargo GPI-CFP. Both proteins are accumulated in the ER during phase 1, and they appear in the same carriers at later time points and during phase 2. No GPI-CFP is found at the plasma membrane, in contrast with neighboring control cells. Arrowheads point at small carriers, arrows at larger intermediates positive for both YT2 and GPI-CFP. Scale bar, 20 μm .

C) The burst of ER export does not depend on the amount of protein synthesized. Golgi biogenesis after complete organelle removal in 9 karyoplast was analyzed with Morphoquant. We derived the total cell F.I. at the time of the start of the ER export burst and considered as max F.I. the plateau level of the total F.I. curve. The chart represents the percentage of the total F.I. at the time when the object F.I. reaches 20% of the max.

D) The GC in phase 3 does not show a preferential position. Radar plot of the location of the GC in phase 3 with respect to its position before laser nanosurgery. 22 karyoplasts were followed by time lapse microscopy and the position of the GC in phase 3 was determined. Positions were then classified into 4 classes (0° , same side of old GC => positions from -45° to $+45^\circ$; $+90^\circ$ => from

+45° to +135°; -90°=> -45° to -135°; 180°, opposite side of the old GC => from +135° to -135°). Values on the axes represent the number of cells with the GC in the corresponding position. The distribution frequency reflects the elongated cell shape and does not show a preferential site for new GC clustering.

Figure S2. Endocytosis during Golgi biogenesis

A) 1-2h after Golgi depletion cells were incubated for 1h in serum-free medium, followed by treatment with Alexa568-labelled transferrin or EGF 2µg/ml for 15 min. Cells were then extensively washed with PBS to remove the non internalized fraction and fixed with PFA. Under this experimental condition, no extracellular EGF or transferrin could be detected (not shown). Confocal z-stacks of images covering the entire cell thickness were acquired and the sum intensity projection is shown for transferrin and EGF. Asterisks indicate the karyoplasts. Scale bars, 20µm.

B) Images obtained as described in A were quantified. After background subtraction, cell outlines were manually segmented and the total F.I. in the cells was quantified and normalized for cell area. In all cases, karyoplasts' values were then divided by the average of control cells in the same image and values for single phase 1 karyoplasts are shown in the plot.

C) Karyoplasts were fixed in phase 1 or 3 and immunostained for the early endosome marker EEA1. Confocal images covering the entire cell thickness were acquired and the projection is shown. Asterisks indicate the karyoplasts. Scale bars, 20 µm.

D) EEA1 clustering index was performed as described in fig.4D and in material and methods. 26, 10 and 7 cells were analyzed for control conditions, karyoplasts ph1 and ph3, respectively. Error bars = s.e.m.

Figure S3. CLEM of YT2 positive structures

A) Time-lapse imaging of Golgi *de novo* biogenesis. After laser nanosurgery, cells were followed by time lapse microscopy until they reached the phase of interest (phase 3 in this case). For an easier visualization, a binucleated karyoplast was chosen. Asterisk = karyoplast; square, round and triangle highlight neighboring cells. These symbols indicate the same cells in B and C. Scale bar, 20 μm .

B) Before fixation higher resolution images of the karyoplast (asterisk) were acquired. The DIC image clearly shows the coverslip etching inside the glass. The outline of the karyoplast's nuclei is shown by the dashed red line for better orientation in the following correlation between light and electron microscopy images. Scale bar, 20 μm .

C) Cell were then fixed, treated with OsO_4 and before embedding the coverslip surface was etched around the karyoplast with a pattern that can be later retrieved on the surface of the resin block as previously reported (Taengemo et al., 2011). This image shows a montage of 3 images that cover the entire area between the etched patterns. The resin block is later trimmed around the groves left with laser etching and serial sections were acquired. Scale bar, 20 μm .

D) The cell of interest is identified by means of particular features of the karyoplast (e.g. the 2 nuclei in this case), the shape of the neighboring cells, as well as the presence of other characteristic features (e.g. glass fragments or cell debris in the area that can be visualized both by light and electron microscopy – arrowheads).

E) Areas of the karyoplast containing interesting YT2 positive structures are identified with the help of cellular shape features and analyzed by EM at different magnification to identify Golgi-like structures or characteristic intermediates (progressive enlargements of the boxed areas).

Scale bars, 20 μm in the LM and low magnification TEM images, 1 μm and 500 nm for the following EM images.

Figure S4. Sec16 colocalizes with sec31 in all the phases of Golgi biogenesis.

A) Karyoplasts were generated by laser nanosurgery and were followed by time-lapse microscopy. At different phases of Golgi biogenesis they were fixed and immunostained for Sec16 and Sec31. Sum projection of Z-stacks covering the entire volume of representative karyoplasts are shown. Insets show enlargements of the boxed area of the karyoplast in the main figure. Scale bars, 10 μ m and 4 μ m in the main figures and insets, respectively.

B) From the images in A the karyoplasts as well as control cells were manually segmented and the colocalization of the sec16 and sec31 labeling was analyzed by the Fiji software using Coloc2 plugin. Scatter plots represent the correlation between the intensities of the pixels in the 2 channels. Pearson's R values for each cell are represented on the plot.

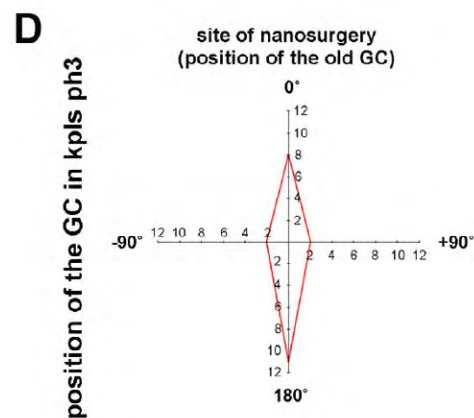
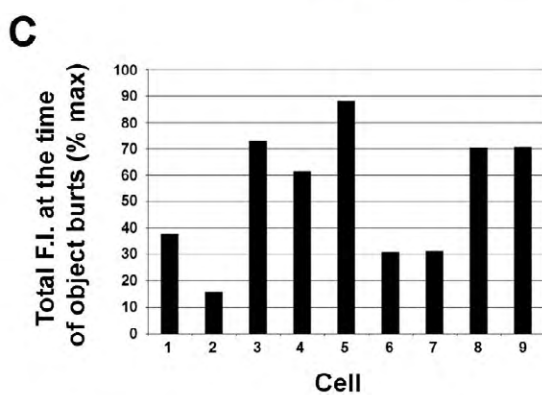
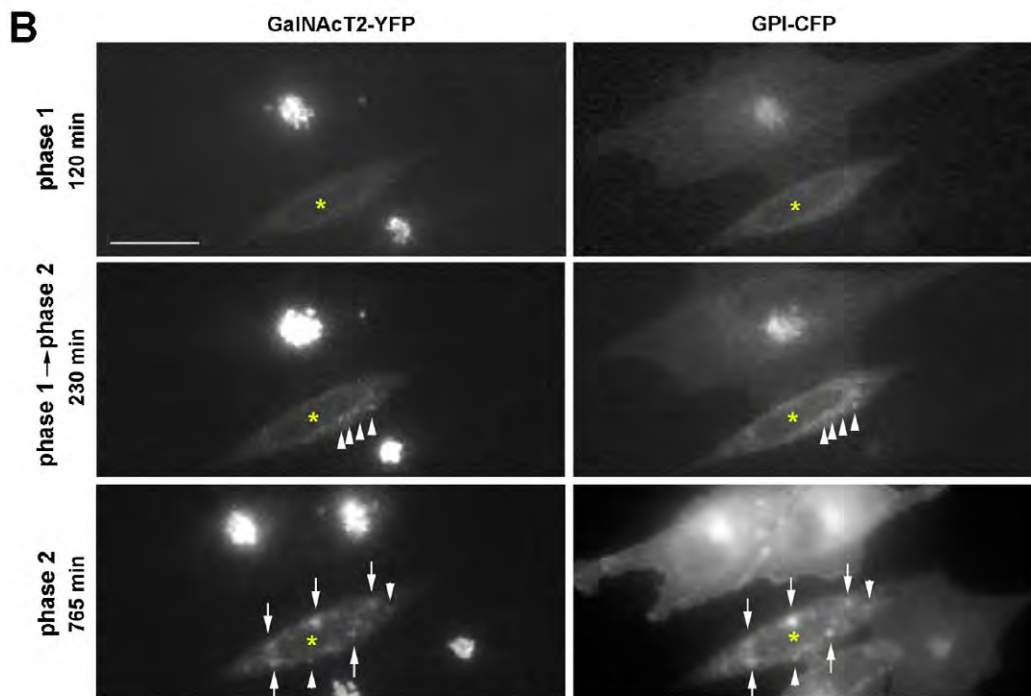
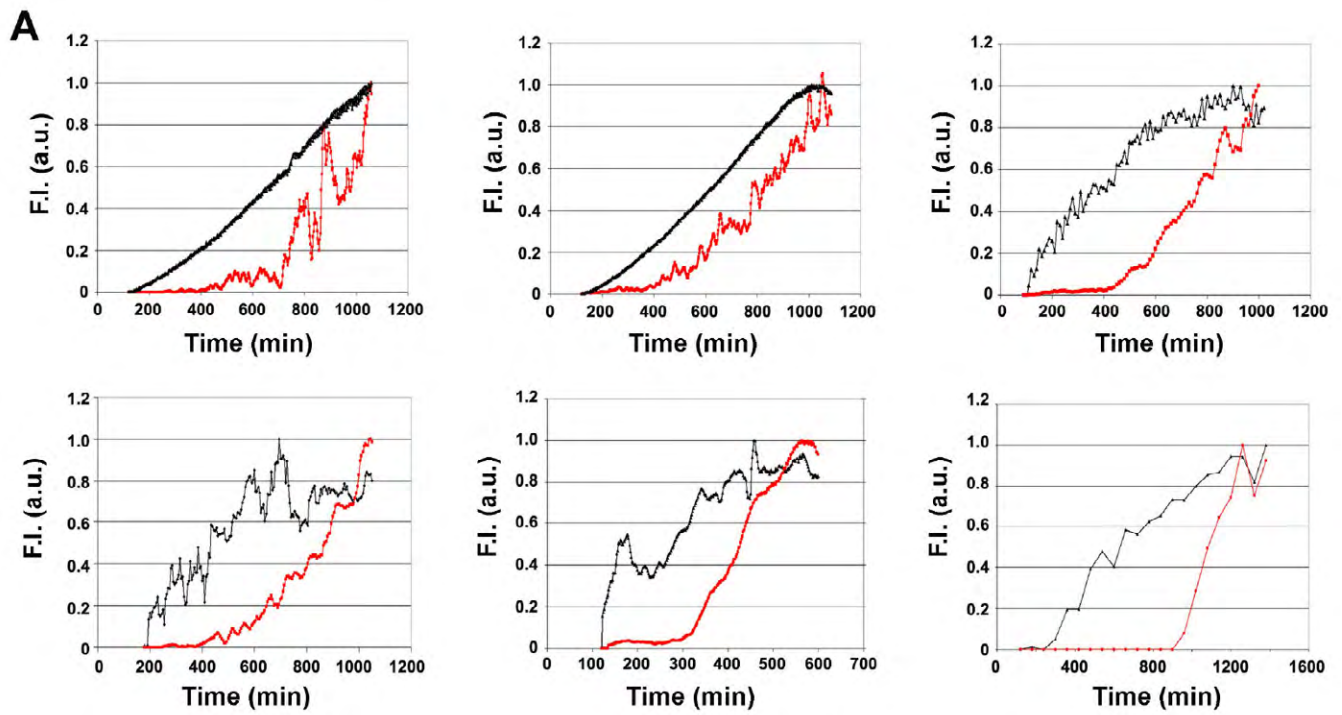


Figure S1

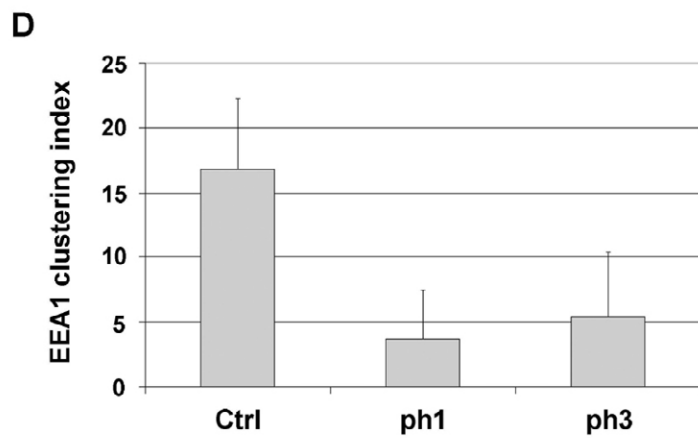
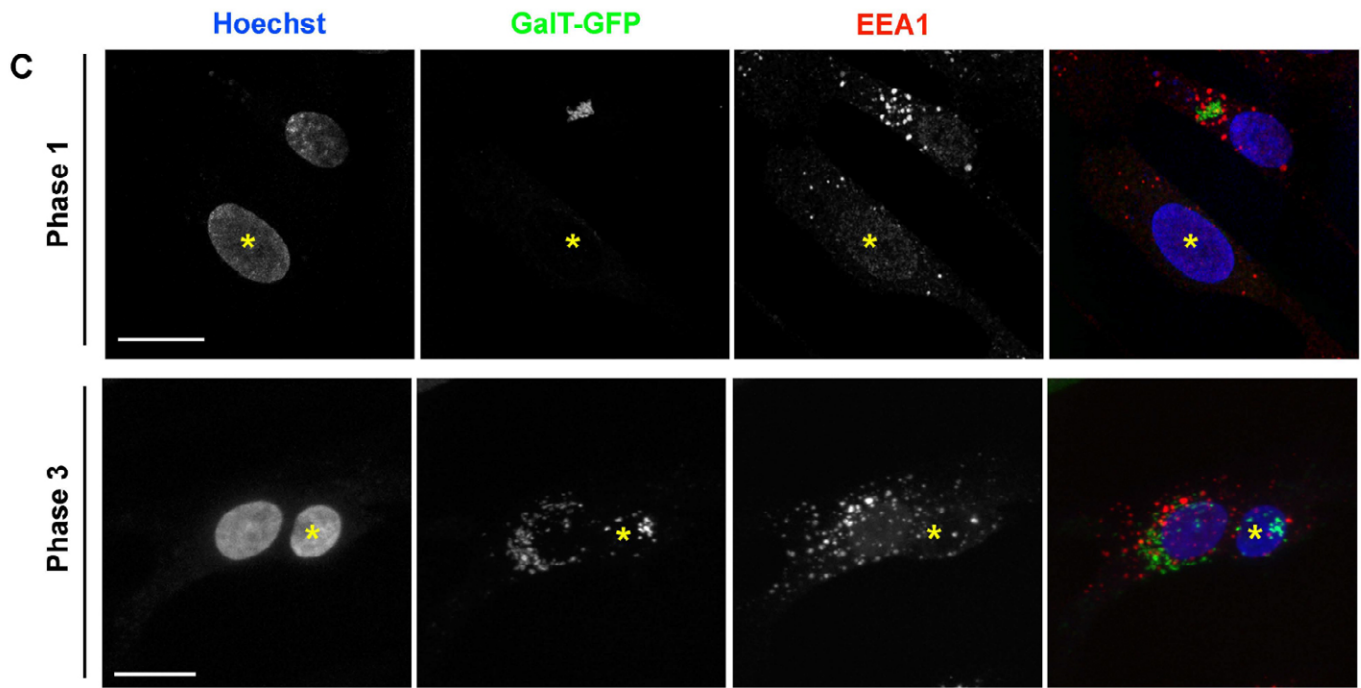
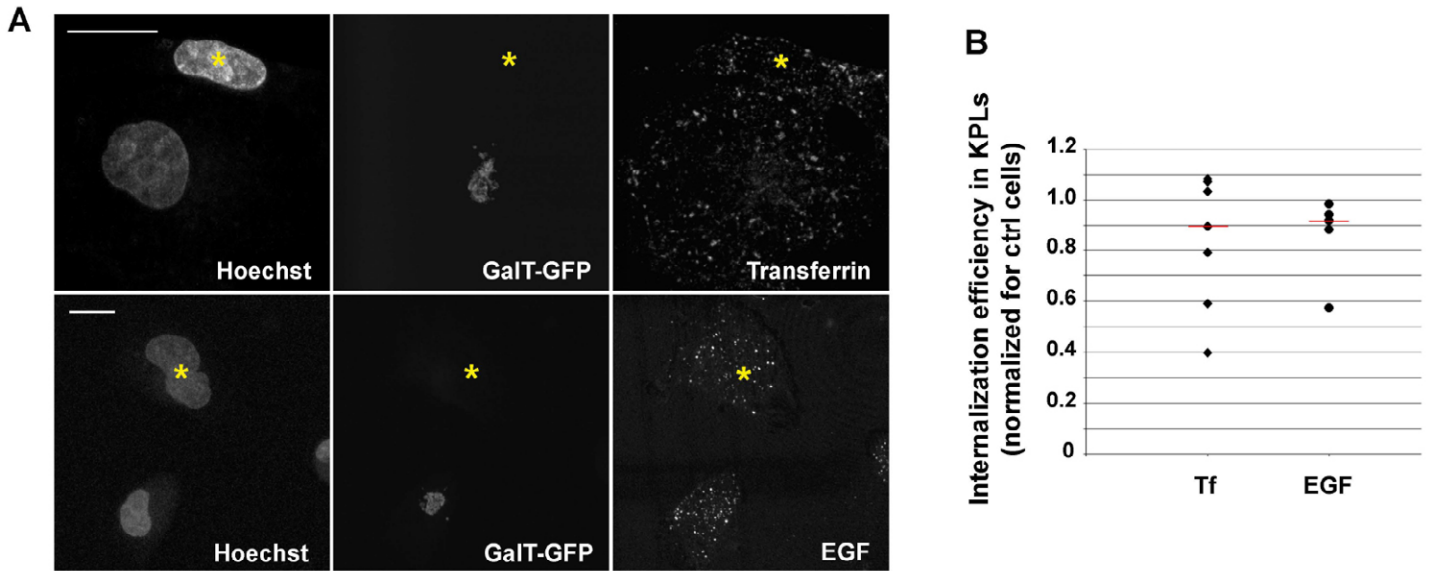


Figure S2

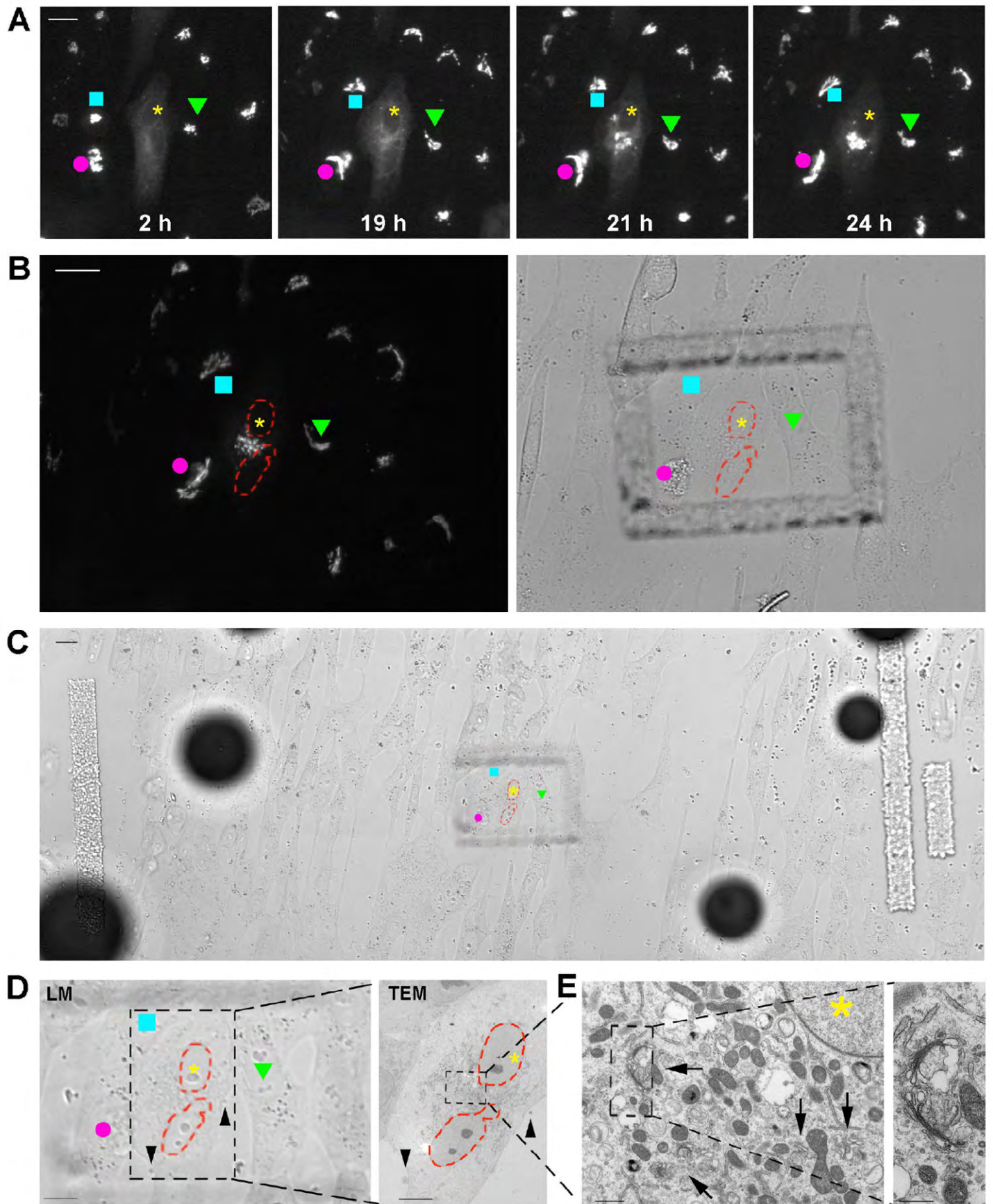


Figure S3

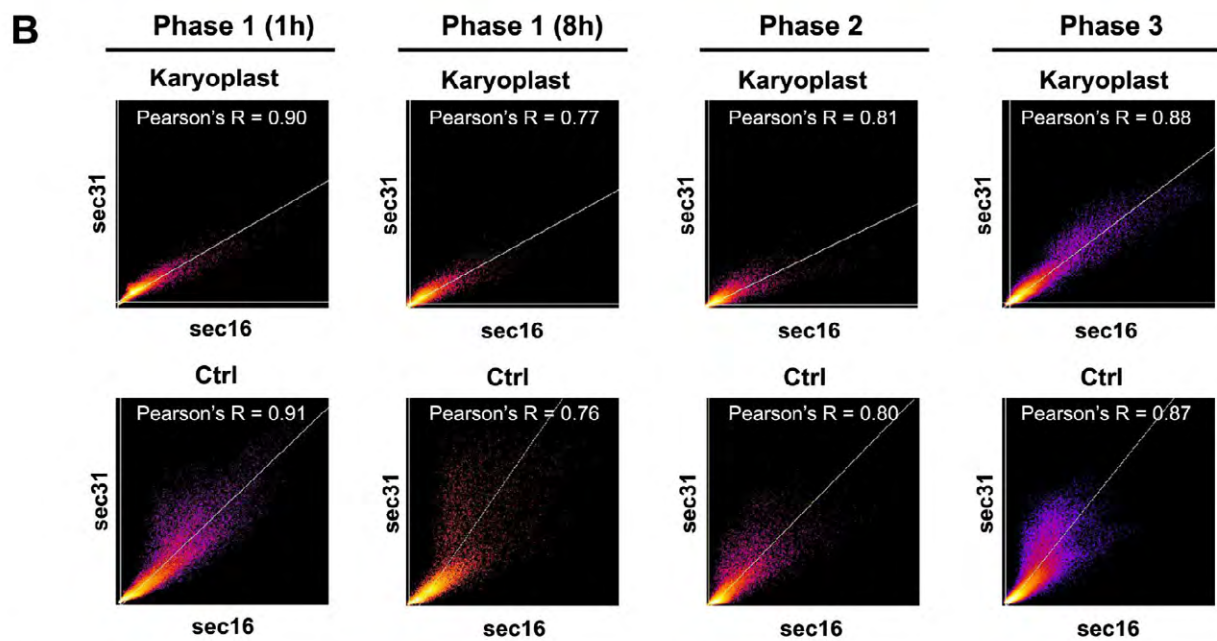
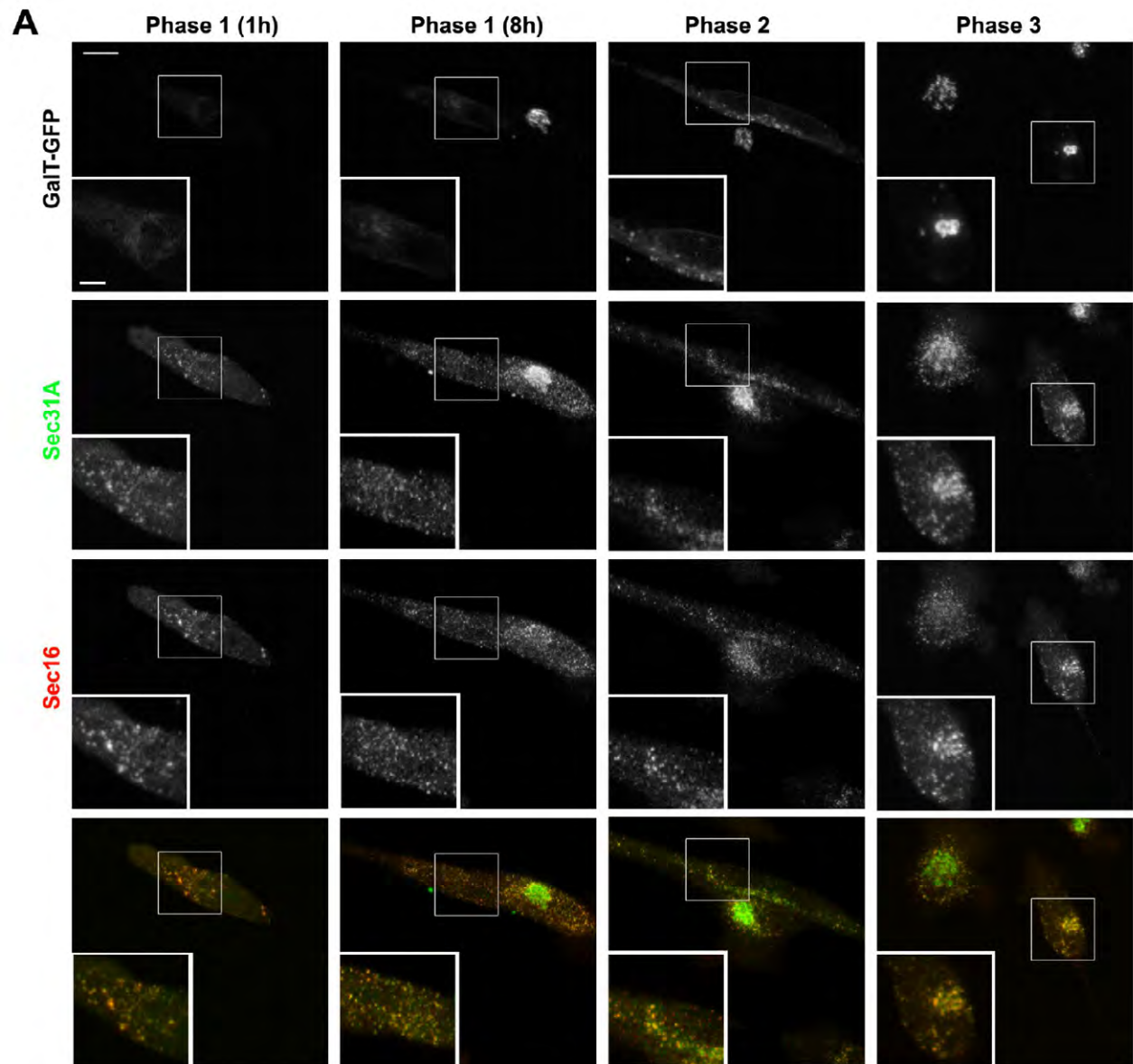


Figure S4



Movie S1. Golgi biogenesis after laser nanosurgery in YT2 cells.

A YT2 cell was dissected by laser nanosurgery in order to completely remove the GC. Golgi biogenesis was subsequently followed by time lapse imaging (2min time resolution). The movie is reproduced with 12min resolution.



Movie S2. Electron tomography of a phase 2 structure

A YT2 cell was dissected by laser nanosurgery and followed by time lapse microscopy until it reached phase 2. The cells were then fixed and embedded for EM. Semi-thin serial sections (300nm) were obtained and tomograms of 3 consecutive sections were acquired with a FEI TECNAI F30 microscope. 3D reconstruction of the tomograms was carried out with the IMOD software. The movie shows the Z-stack of tomographic slices and the 3D reconstruction of a Golgi precursor structure. Each color represents a continuous membrane-bounded structure.